Flow past triangular cylinder

Thanakorn Chanthanasaro

(January 12, 2018)

Running head: **Flow past triangular cylinder**

ABSTRACT

Flow over triangular cylinder is simulated using OpenFOAM at Reynold number(Re) 40 and 156. The incompressible Navier-Stokes equations are used in the simulation. The flow past triangular cylinder at Re = 40 shows no vortex shedding behind the cylinder. Where vortex shedding is observed for Re = 156. The lift and drag coefficients are investigated. The pressure at the location far from the cylinder is also plotted. However, there is no results of acoustical properties yet.

Introduction

Aeroacoustics is the field that studies the sound generated by the fluid either the turbulence of the fluid or the force fluctuation of the fluid on the rigid body, for example. The simple examples of this kind of sound are sound from wind instruments, or Aeolian tone which is the tone produced by wind blowing over fixed objects. The aeroacoustics has became more popular because it can be used to reduce the noise for example, in automotive industry, aeronautics or high speed train.

In 1952, James H. Lighthill published the first paper about sound generated aerodynamically Lighthill (1952). He rearranged the Navier-Stokes equations into the inhomogeneous wave equation called Lighthill's equation.

$$\left(\frac{\partial^2}{\partial t^2} + \boldsymbol{\nabla}^2\right)(c_0^2(\rho - \rho_0)) = \frac{\partial^2 T_{ij}}{\partial x_i \partial x_j} \tag{1}$$

where

$$T_{ij} = \rho u_i u_j + \delta_{ij}((p - p_0) - c_0^2(\rho - \rho_0)) - \tau_{ij} \tag{2}$$

is Lighthill stress tensor. The subscript "0" represent the referenced value, ρ is density, p is pressure, u_i is the fluid velocity in i-direction, c_0 is speed of sound, and τ_{ij} is viscous stress tensor.

Lighthill's equation is the linear wave equation of fluctuating density (sometimes expressed as acoustic pressure) where the right hand side of the equation contains the sound source term. The main idea of Lighthill's equation is to describe the propagation of sound in a quiescent medium with sound speed c_0 surrounding the source region. In that paper, he gave the solution to his equation using the Green's function as

$$\rho(\mathbf{x},t) - \rho_0 = \frac{1}{4\pi c_0^2}\frac{\partial^2}{\partial x_i \partial x_j}\int T_{ij}\left(\mathbf{y}, t - \frac{|\mathbf{x}-\mathbf{y}|}{c_0}\right)\frac{d\mathbf{y}}{|\mathbf{x}-\mathbf{y}|} \tag{3}$$

where the integral is taken over the source region. The limit of this solution is it can be used only for unbounded fluid where no rigid surface exist. Curle (1955) and J. Williams (1969) later extended the solution to include the effect of stationary rigid surface and moving surface respectively by adding the surface integral terms. For most cases, the Lighthill stress tensor can be approximated by only the first term of the tensor $T_{ij} \approx \rho u_i u_j$ and is associated with quadrupole sound source. Whereas the directivity pattern for the force fluctuation at the surface is associated with dipole source.

Methods

The 2D simulation of flow over bluff bodies are investigated using OpenFOAM (Open Source Field Operation and Manipulation). There are three different bluff bodies I used which are circular cylinder and triangular cylinder. For the circular cylinder case, I brought the entire thing from website "http://the-foam-house5.webnode.es". And for the other cases, I modified the geometry of the circular cylinder case to other shapes. The solver I used in this report is `icoFoam` which is the solver for solving the incompressible laminar Navier-Stokes equations using the PISO algorithm (I will change to the compressible solver in the future). The governing equations for incompressible flow are given by

$$\nabla \cdot \mathbf{u} = 0 \tag{4}$$

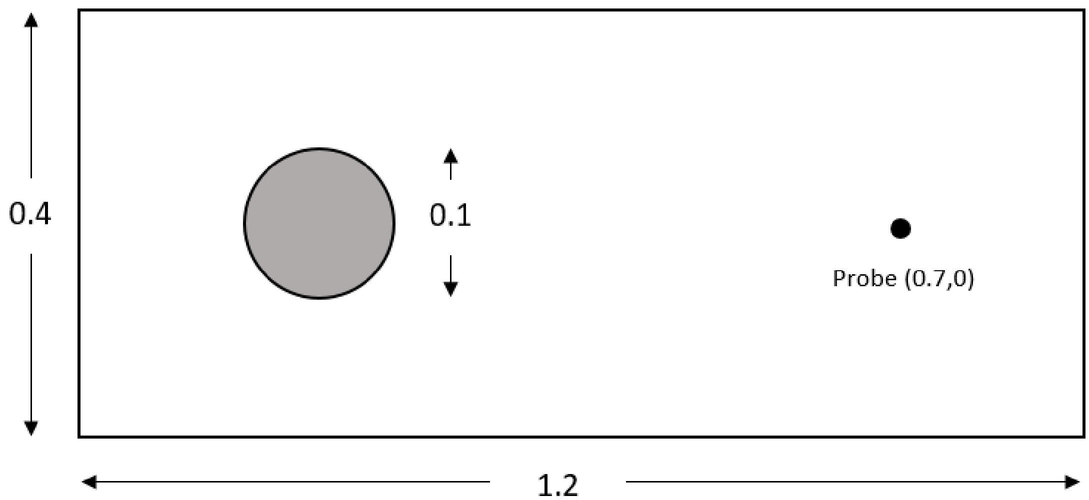

Figure 1: The geometry of the simulation of flow past circular cylinder (not to scale).

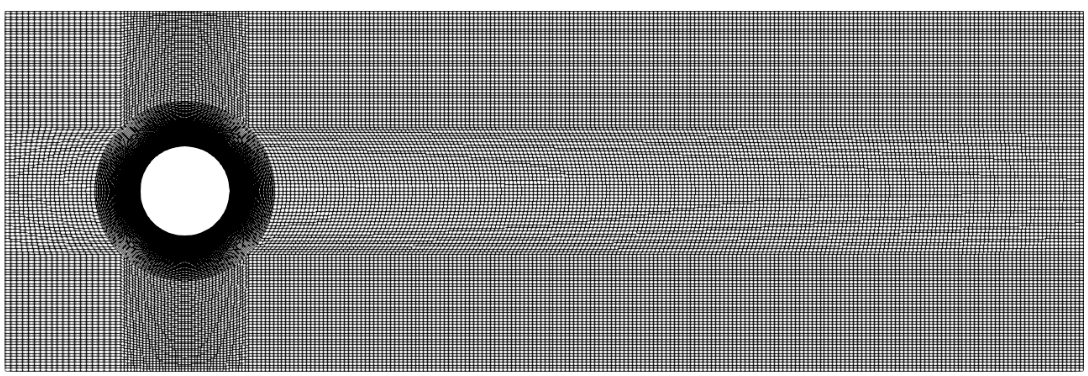

Figure 2: The computational mesh of flow past circular cylinder.

$$\frac{\partial \mathbf{u}}{\partial t} + (\mathbf{u} \cdot \nabla)\mathbf{u} - \nu \nabla^2 \mathbf{u} = -\frac{1}{\rho} \nabla p \tag{5}$$

where $\mathbf{u}$ is velocity vector, ν is kinematic viscosity, ρ is density, and p is pressure. The geometry of computational domain and computational mesh are shown in figure 1 and 2. The size of the computational domain is 1.2×0.4. The center of the cylinder is placed at the origin.

For the flow past triangular cylinder, the computational mesh is shown in figure 5

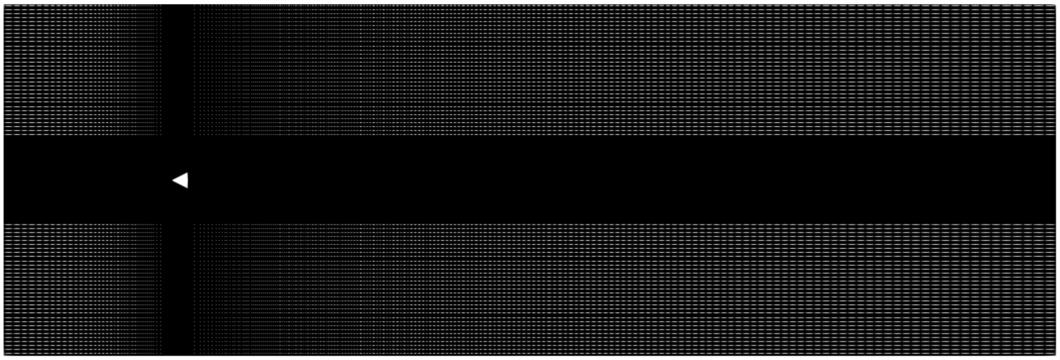

Figure 3: The computational mesh of flow past triangular cylinder.

Results

Currently, I do not have result of acoustical properties of the flow simulation yet. The acoustical properties of the flow that researchers often put into their papers are directivity pattern of root mean square of acoustic pressure, contour of instantaneous acoustic pressure, and sound spectra, for example. I will be trying to get those results in the future. For now, I have drag coefficient, lift coefficient (since these two coefficients are related with the sound generated), flow characteristic, and the value of pressure at the location of probe showing in figure 4-15.

For flow past circular cylinder, the magnitude of velocity field at time t = 1.75 s is shown in figure 4. Vortex shedding is observed behind the cylinder at later time. The lift and drag coefficients in figure 5 and 6 start oscillating around time $t \approx 1.2$ s due to the vortex shedding. The pressure at the probe location is plotted in figure 7.

For flow past triangular cylinder at Re = 40, the magnitude of velocity field at time $t = 1$ s is shown in figure 8. There is no vortex shedding observed behind the cylinder due to the very low Reynold number. The lift and drag coefficients are shown in figure 9 and 10. The lift coefficient shows some oscillation but the value is very small (in order of 10^{-7}).

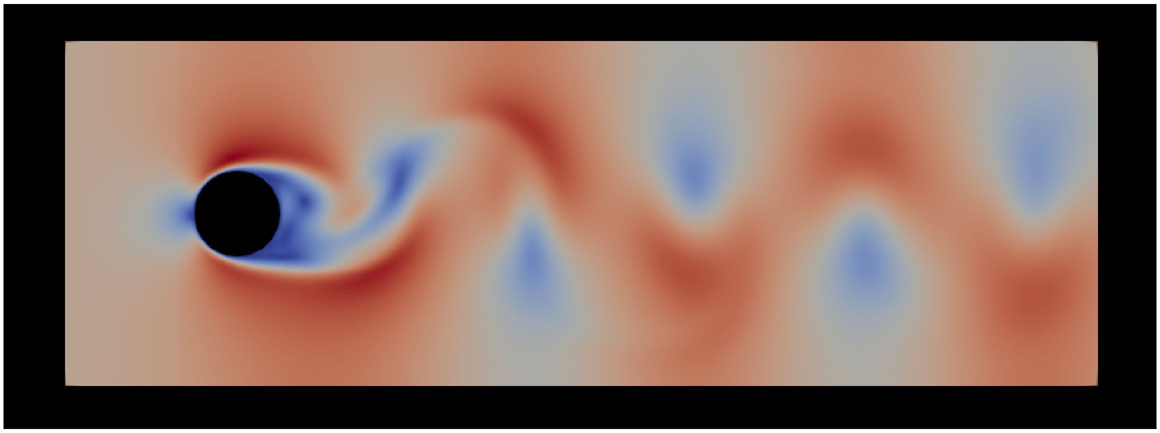

Figure 4: The plot of velocity magnitude of flow past circular cylinder versus time at Re 195 at $t = 1.75$ s.

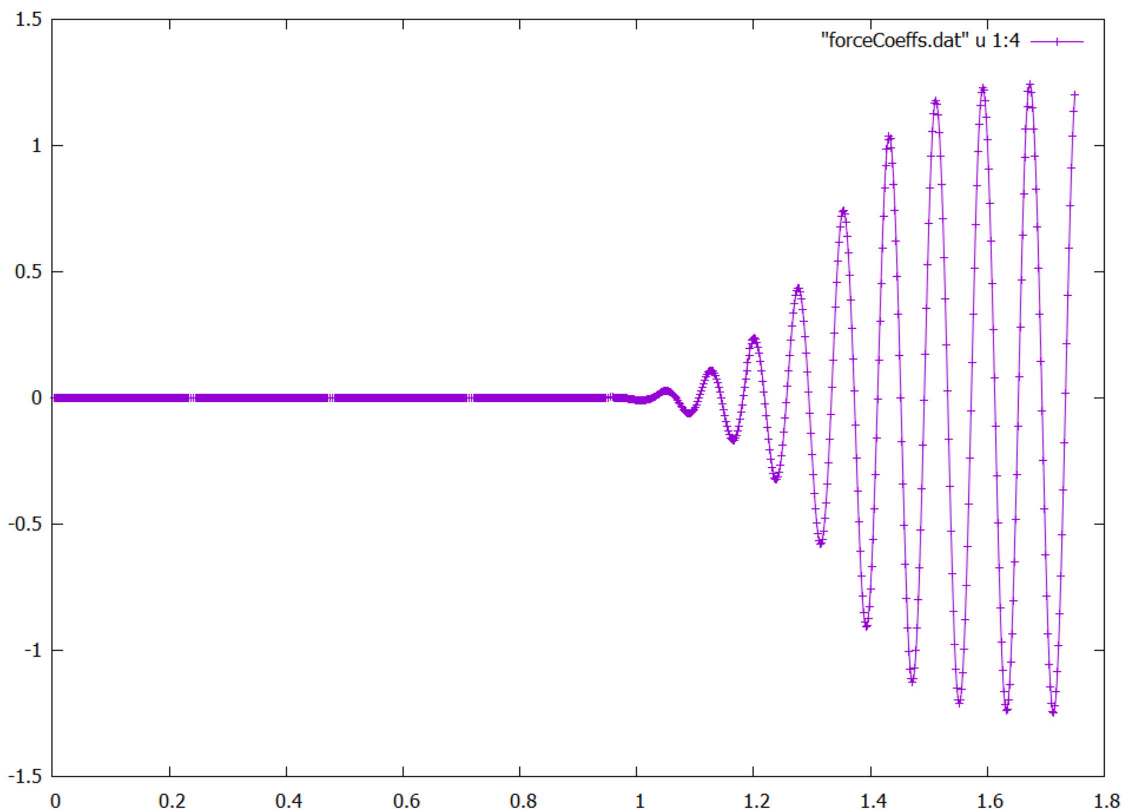

Figure 5: The plot of lift coefficient of flow past circular cylinder versus time at Re 195.

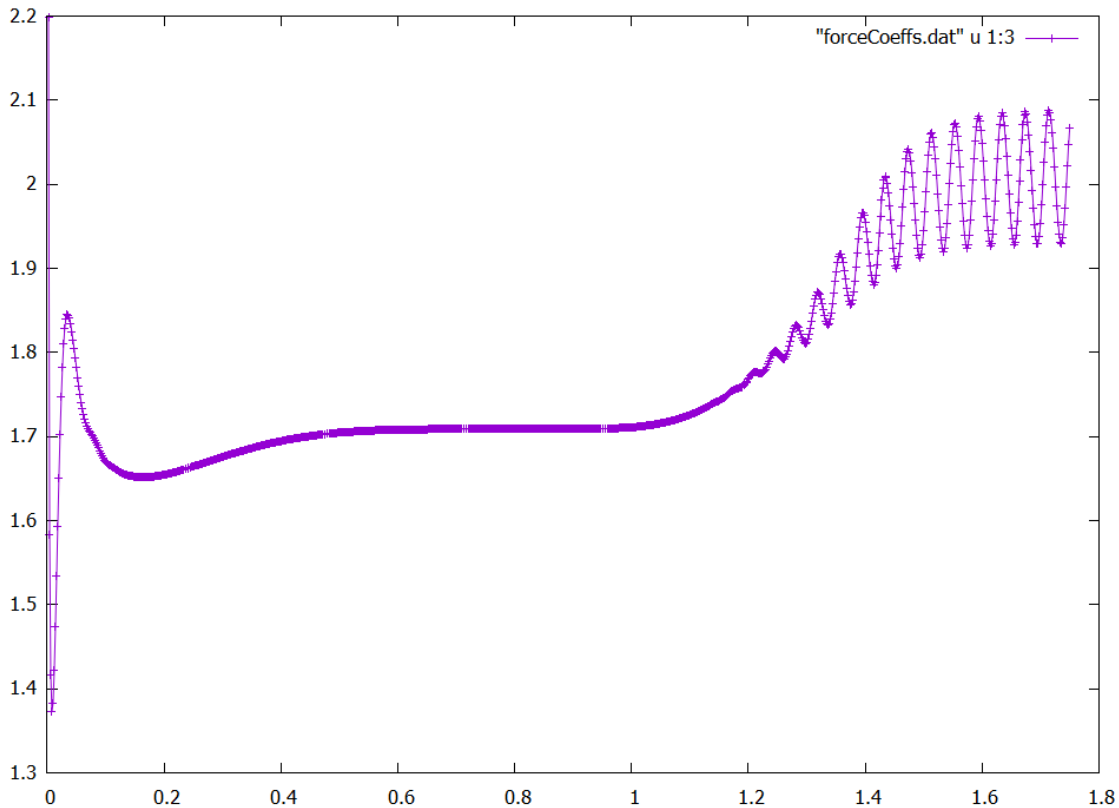

Figure 6: The plot of drag coefficient of flow past circular cylinder versus time at Re 195.

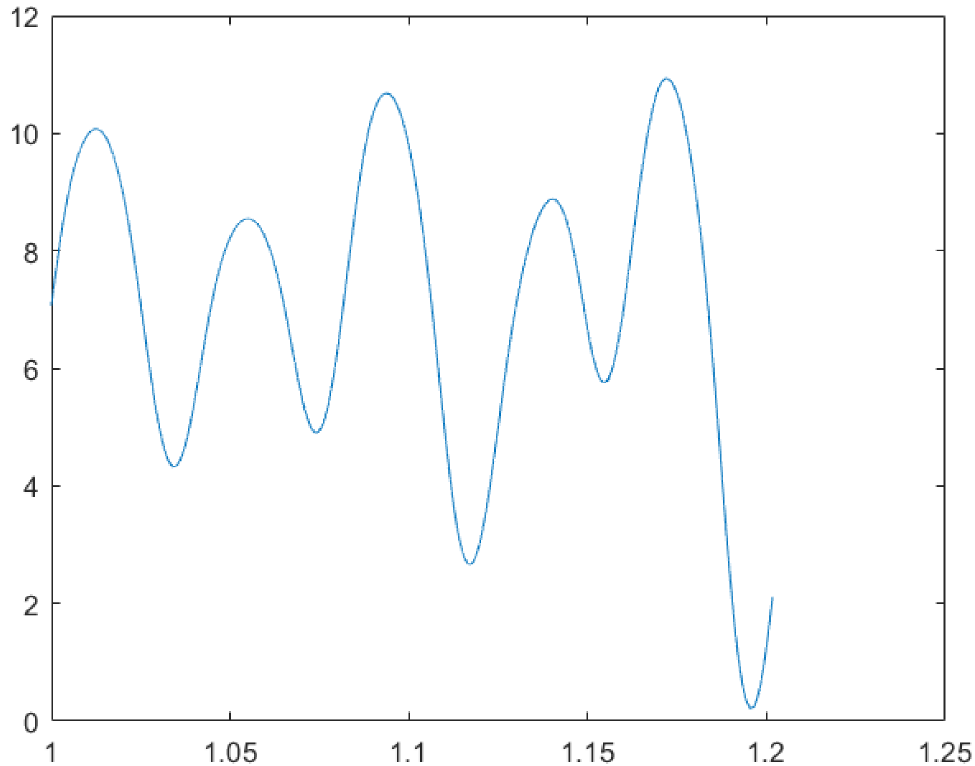

Figure 7: The plot of pressure coefficient of flow past circular cylinder versus time at Re 195.

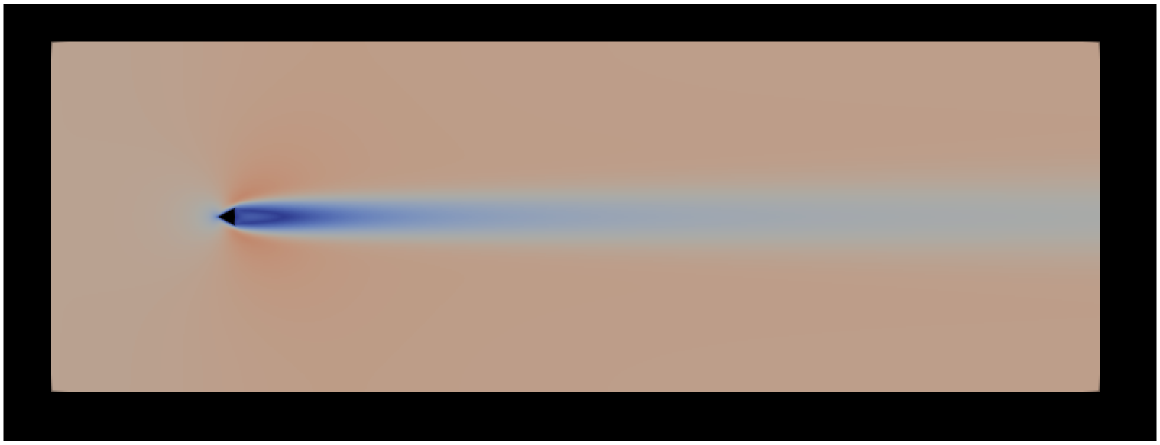

Figure 8: The plot of velocity magnitude of flow past triangular cylinder versus time at Re 40 at $t = 1$ s.

There is also no oscillation in drag coefficient and the value is about 0.32. The pressure at the probe location is plotted in figure 11.

For flow past triangular cylinder at Re = 156, the magnitude of velocity field at time $t = 1$ s is shown in figure 12. Vortex shedding is observed behind the cylinder. The lift and drag coefficients are shown in figure 13 and 14 showing some complicated pattern. The pressure at the probe location is plotted in figure 15.

Discussion

The flow over triangular cylinder is simulated. The first thing I want to point out is that I used incompressible solver to simulate flow in this report but I think I should use compressible solver to solve the acoustics problem. Second, I don't think my meshing for flow past triangular cylinder is good enough. So, I will fix that later. Third, after fixing the computational mesh, I will start getting the acoustical properties such as, directivity pattern, sound spectra, or contour of acoustic pressure. Fourth, I will start studying the effect of angle of stream direction and triangular cylinder on the acoustic properties of the

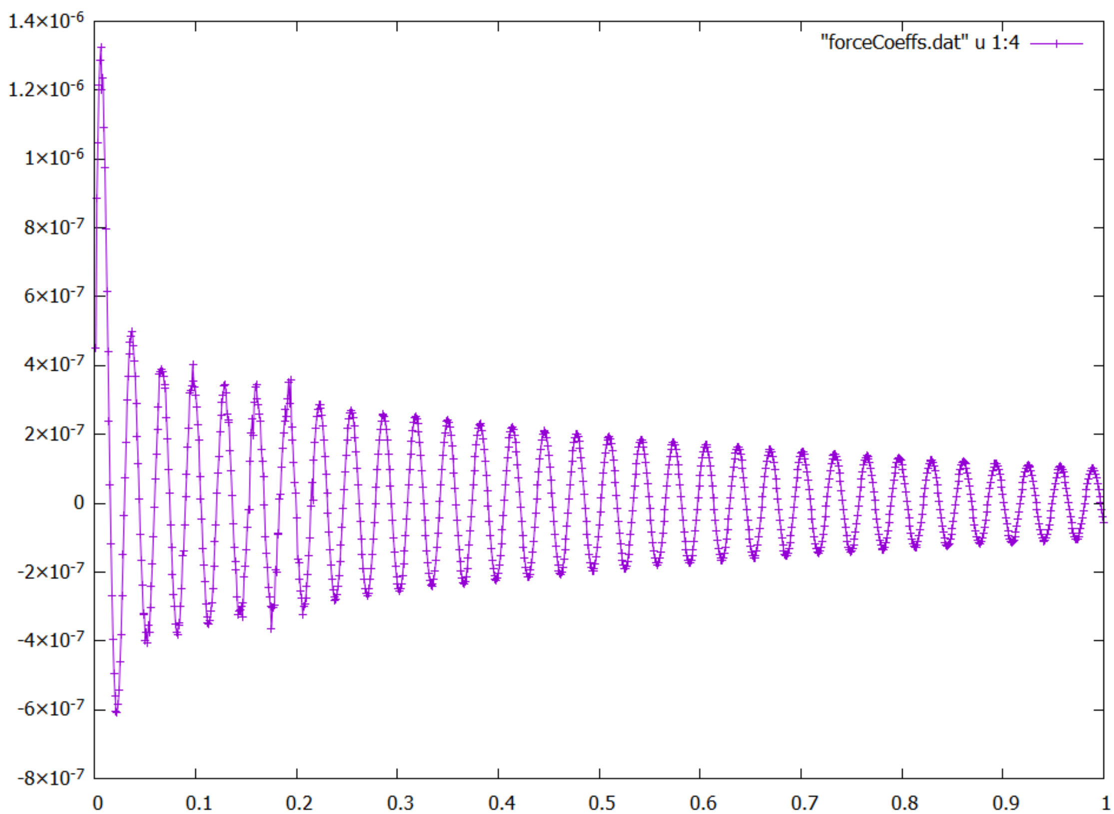

Figure 9: The plot of lift coefficient of flow past triangular cylinder versus time at Re 40.

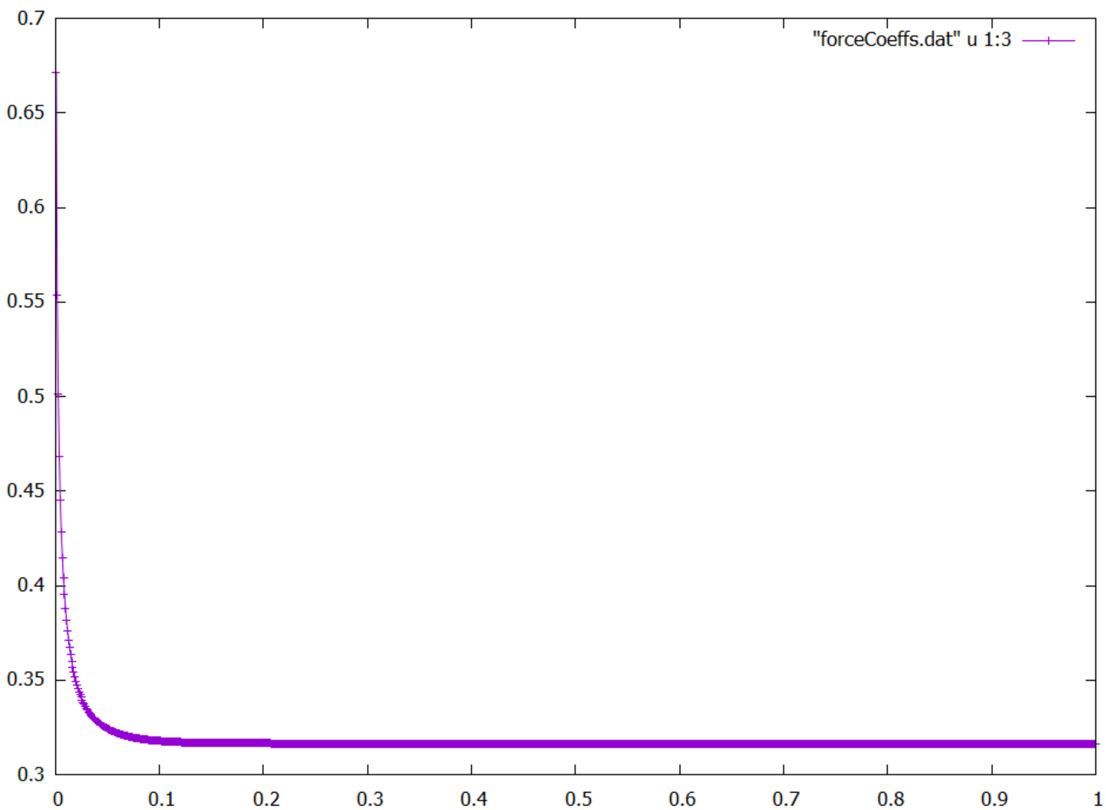

Figure 10: The plot of drag coefficient of flow past triangular cylinder versus time at Re 40.

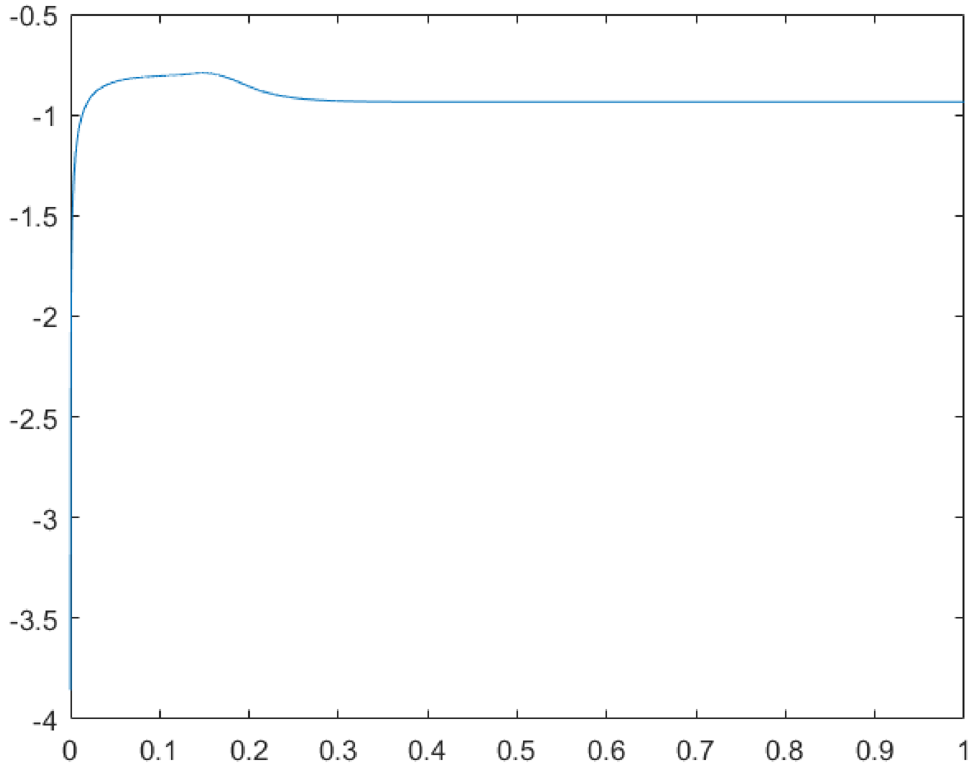

Figure 11: The plot of pressure of flow past triangular cylinder versus time at Re 40.

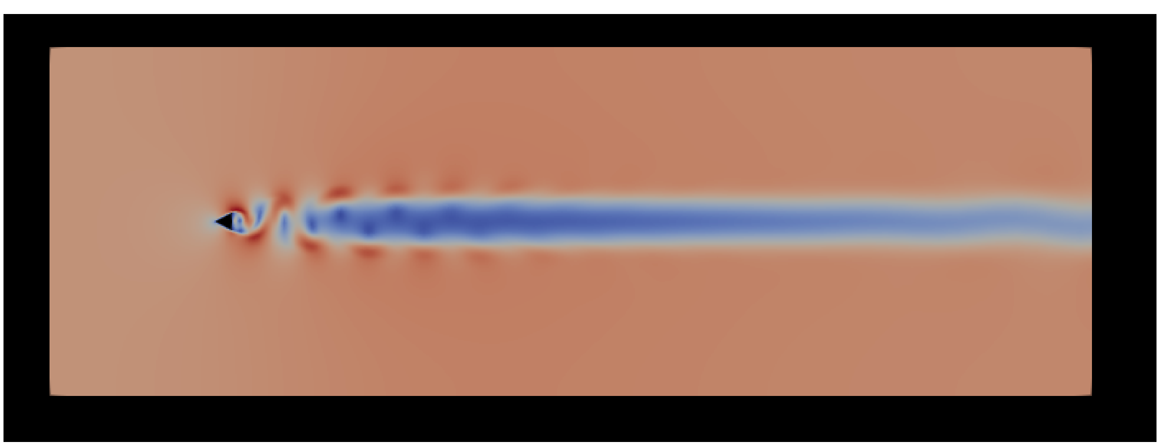

Figure 12: The plot of velocity magnitude of flow past triangular cylinder versus time at Re 156 at $t = 1$ s.

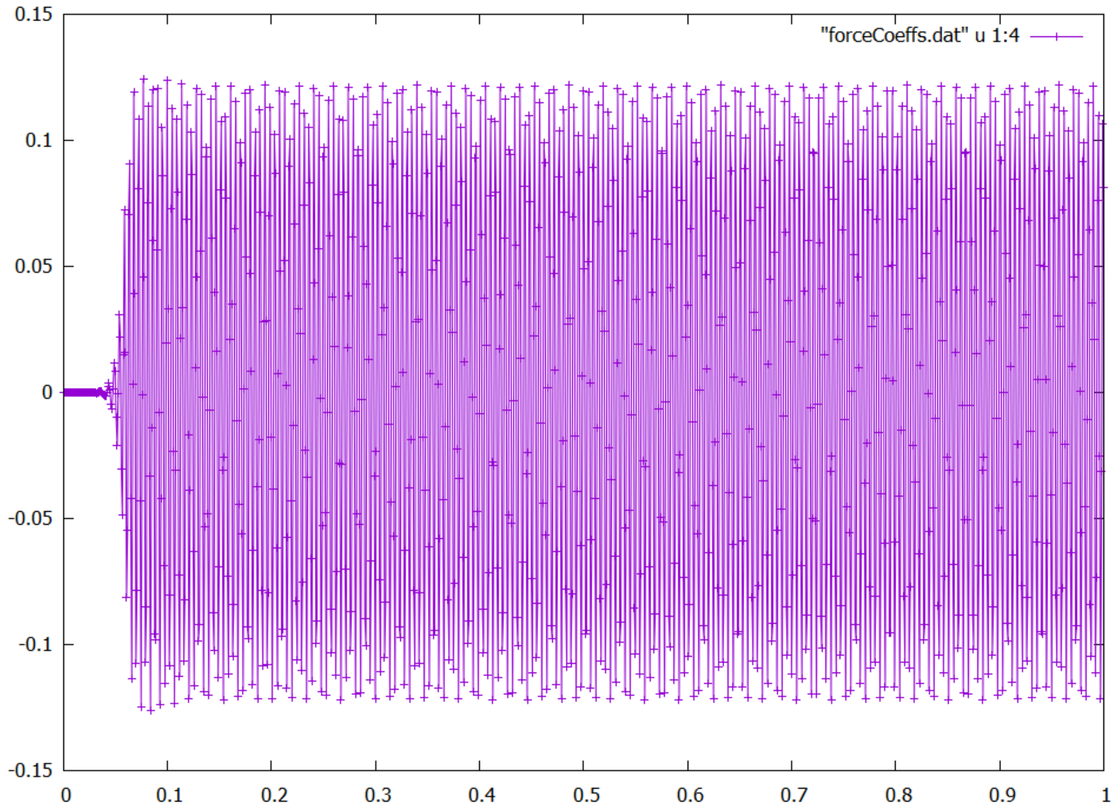

Figure 13: The plot of lift coefficient of flow past triangular cylinder versus time at Re 156.

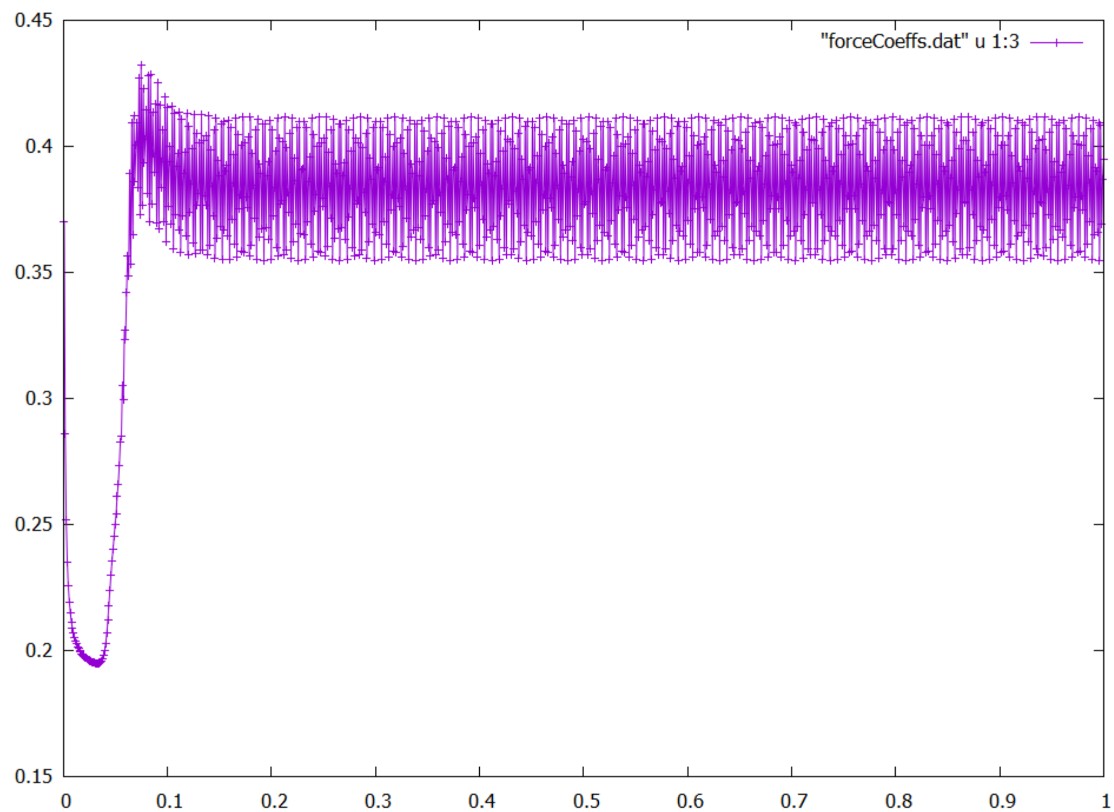

Figure 14: The plot of drag coefficient of flow past triangular cylinder versus time at Re 156.

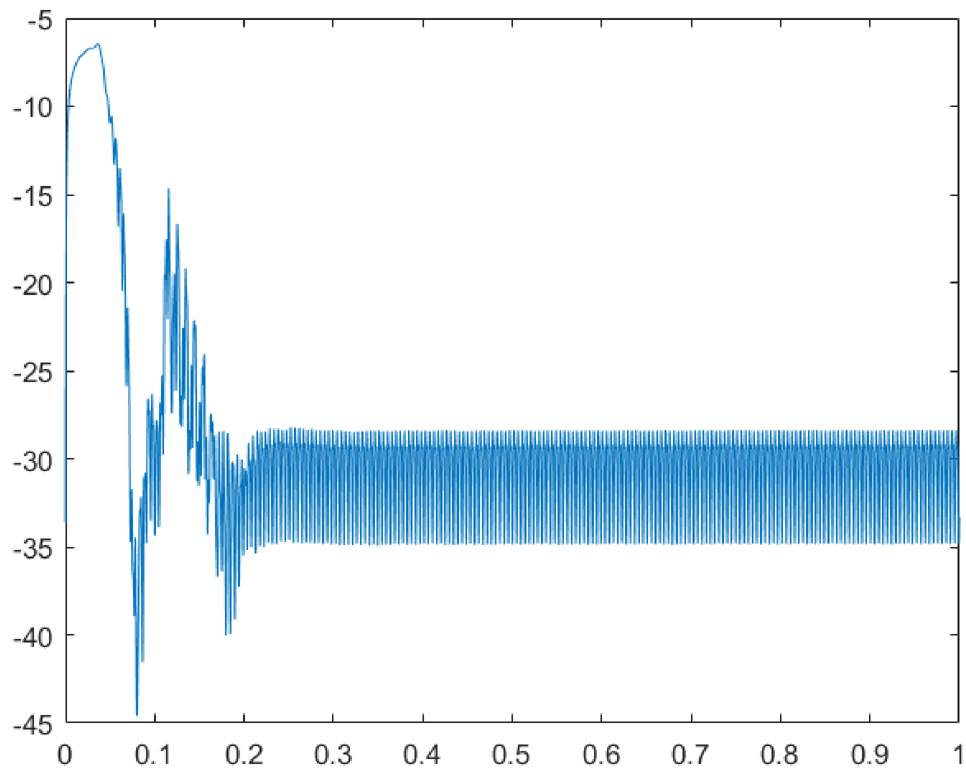

Figure 15: The plot of pressure coefficient of flow past triangular cylinder versus time at Re 156.

flow. The 3D simulation and high Re simulation are also considered.

Conclusion

The 2D simulation of flow over circular cylinder and triangular cylinder are investigated. For flow past circular cylinder at Re = 195 and flow past triangular cylinder at Re = 156, vortex shedding is observed behind the cylinder. There is no vortex shedding observed in flow past triangular cylinder at Re = 40. Lift and drag coefficients of each case are carried out because they are related with the sound generated. The acoustical properties will be carried out in the future (if possible).

REFERENCES

Curle, N., 1955, The influence of solid boundaries upon aerodynamics ound: Proceedings Of The Royal Society A:Mathematical, Physical And Engineering Sciences, **231**, 505–514.

J. Williams, D. H., 1969, Sound generation by turbulence and surfaces in arbitrary motion: Philosophical Transactions Of The Royal Society A:Mathematical, Physical And Engineering Sciences, **264**, 321–342.

Lighthill, M., 1952, On sound generated aerodynamically. i.general theory: Proceedings Of The Royal Society A:Mathematical, Physical And Engineering Sciences, **211**, 564–587.